

## Seasonal Variation of Water Content and Pore-water Pressure Distribution in Vegetated Soil Slope

N. Gofar<sup>1</sup>, H. Rahardjo<sup>1</sup>, A. Satyanaga<sup>1</sup>

<sup>1</sup>School of Civil and Environmental Engineering, Nanyang Technological University, 50 Nanyang Avenue, Singapore. 639798.  
E-mail: nurlygofar@ntu.edu.sg

**ABSTRACT:** This paper presents soil water content and pore-water pressure distribution in a vegetated residual soil slope in response to a one-year seasonal variation in Singapore. The measurements were taken by tensiometers and soil moisture sensors TM1-SM1, TM2-SM2, TM3-SM3 and TM4-SM4 installed at vertical distances of 2.0, 2.0, 1.37 and 0.23 m from slope surface. Seasonal variation was represented by rainfall and actual evaporation calculated based on data collected by a weather station installed at the site. The field monitoring shows that the soil water content and pore-water pressure measurements by TM1-SM1, TM2-SM2, TM3-SM3 were representative of soil-water characteristic curve (SWCC) of the residual soil. On the other hand, the measurements by TM4-SM4 shows a lower pore-water pressure during dry period and a lower volumetric water content during wet period as compared to SWCC of residual soil. The study showed that the response recorded by TM4-SM4 was representative of top soil used as media for vegetation planting. The study also showed that bigger variation of pore-water pressure recorded by TM4 in December 2016 and January 2017 was due to long dry period with high temperature which is not normal in Singapore during these months.

**Keywords:** Field monitoring, soil water content, pore-water pressure, soil-water characteristic curve, vegetated soil slope.

### 1. INTRODUCTION

Soils in tropical regions commonly consist of residual soils with negative pore-water pressure in the zone above ground water table (Rahardjo et al. 2005). The pore-water condition is influenced by flux boundary conditions such as rainfall, evaporation, and transpiration processes. Earlier studies consider only rainfall as the flux boundary condition to avoid more complexity in their analysis of pore-water pressure and slope stability (e.g. Chipp et al., 1982; Rahardjo et al., 1998; Ng et al., 2003; 2008 and Li et al., 2005; Lee et al., 2008). However, not all rainfall becomes infiltration. From the definitions, the rainfall may be separated into four components, i.e. runoff, infiltration, interception (rainfall that is caught on the vegetation surfaces), and evapotranspiration (ET) (Joel et al., 2002). Thus, some researchers took further steps to consider the portion of precipitation that infiltrates into the soil (Ng et al. 2003; Rahardjo et al. 2005; Gofar et al. 2008). Other researchers also consider the effect of evaporation on the prediction of pore-water pressure variation in soil slope (e.g. Gasmo et al., 2000; Gitirana et al., 2005 2006; Yunusa et al., 2014). Numerical analysis performed by Yunusa et al. (2014) on one-year data showed a better agreement with field response of unsaturated soil when the input data was the combination of rainfall and evaporation rates. Rahardjo et al (2017) included the effect of evapotranspiration in their study of pore-water pressure variation in vegetated soil slope. These studies suggested rainfall and evaporation as well as transpiration play important roles in affecting the pore-water pressure distribution within residual soil slope.

The response of the soil to flux boundary conditions can be evaluated by field monitoring of the flux boundaries as well as the transient volumetric water content and pore-water pressure in the soil. The intensity of rainfall that falls on the slope is normally monitored using a tipping-bucket rain gauge. In contrast to rainfall, evapotranspiration rate from vegetated surface cannot be easily measured. Potential evaporation rate ( $PE$ ) can be measured in the field using Lysimeter or predicted based on climate data (Penman, 1948) equation. The  $PE$  is an evaporation from an open water body whereby the relative humidity is equal to unity. The actual evaporation ( $AE$ ) from a soil surface is related to the relative humidity in the soil at ground surface is about 70% of the  $PE$  (Sattler and Fredlund, 1991).

In addition to the relative humidity of soil surface, transpiration should be considered for the effect of flux boundary conditions on vegetated surface. Several empirical methods are available to obtain evapotranspiration ( $ET$ ) rate. Weather station can be installed to capture the meteorological variables required to calculate the evapotranspiration such as air temperature, solar radiation, relative humidity and wind speed (Rahardjo et al., 2014). Allen (1998)

recommended the use of updated Penman-Monteith Method or FAO-56 Method (Zotarelli et al, 2009) to calculate the rate at which readily available soil water is vaporized from a specified vegetated surface  $ET_o$ . The effect of different species of vegetation can be considered by modifying the equation with a crop coefficient,  $K_c$  (Lazzara and Rana, 2010), thus ( $ET_c = ET_o \times K_c$ ).

The transient volumetric water content and pore-water pressure in soil are measured by soil moisture sensor and tensiometer respectively. The state of moisture in the unsaturated zone of soil between the ground surface and the water table (Blight, 1997) is controlled by the water balance between the water input into water output from the soil. The change in water stored in soil lead to the change in both volumetric water content and pore-water pressure. Long term real-time monitoring is required to capture the effect of different weather conditions throughout the year.

The water flow into the soil is governed by the coefficient of permeability with respect to water ( $k_w$ ) (Fredlund and Rahardjo, 1993). Unlike saturated soils, the permeability of an unsaturated soil is a non-linear function of the volumetric water content of the soil. When the soil approaches saturation, the permeability becomes constant and equal to the saturated coefficient of permeability,  $k_s$ . Thus, the response of soil to the flux boundary conditions is controlled by the soil water characteristic curve (SWCC) which is non-linear with respect to the negative pore-water pressure (suction). In other words, the ability of the unsaturated soil to retain water varies with soil suction. The SWCC follows different paths during drying and wetting (hysteresis) in nature. The soil on the drying path has a higher water content than the soil on the wetting path at a given matric suction. Thus, the field data of volumetric water content and pore-water pressure could be plotted within the hysteretic of the drying and wetting curves of the SWCC.

This paper presents response of residual soil slope to flux-boundary conditions based on field monitoring data collected from an instrumented slope in Singapore. The rainfall data collected by rain-gauge and evapotranspiration ( $ET_c$ ) were used as flux boundary conditions while the responses were identified by volumetric water content and pore-water pressure recorded by soil moisture sensor and tensiometers. The responses were compared to the soil-water characteristic curve (SWCC) of the corresponding soil surrounding the soil moisture sensors and tensiometers tip.

### 2. THEOTERICAL BACKGROUND

The evaporation from ground surface covered with certain species of vegetation ( $ET_c$ ) can be calculated by considering standard meteorological variables and a crop coefficient ( $K_c$ ) (Lazzara and Rana 2010), thus  $ET_c$  is calculated as follows:

$$= \times \quad (1)$$

where  $ET_o$  is the reference evapotranspiration in mm/day which can be calculated as follows:

$$= \frac{0.408 \Delta ( - ) + \gamma \left( \frac{900}{+273} \right)^2 ( - )}{\Delta + \gamma (1 + 0.34 - 2)} \quad (2)$$

where  $T$  = mean air temperature ( $^{\circ}\text{C}$ );  $u_2$  = wind speed (m/s) at 2 m above the ground;  $R_n$  = net radiation flux ( $\text{MJ}/\text{m}^2/\text{day}$ );  $G$  = sensible heat flux into the soil ( $\text{MJ}/\text{m}^2/\text{day}$ );  $e_s$  = saturation vapour pressure (kPa);  $e_a$  = actual vapor pressure (kPa);  $\Delta$  = slope of saturation vapour pressure curve; and  $\gamma$  = psychrometric constant. The detailed calculation of this method can be found in Zotarelli et al. (2009). Typical  $K_c$  values are given in Lazzara and Rana (2010), for grass,  $K_c = 1$ .

The water flow through an isotropic unsaturated soil is formulated using Darcy's law as follows (Fredlund and Rahardjo, 1993):

$$- \left( \frac{h}{\rho} \right) + - \left( \frac{h}{\rho} \right) = \frac{1}{2} \rho g \frac{h}{\rho} \quad (3)$$

with

$$h = \frac{p}{\rho g} + z \quad (4)$$

where  $h_w$  = hydraulic head;  $z$  = elevation head;  $u_w$  = pore-water pressure (kPa);  $x$  and  $y$  are the Cartesian coordinates in the  $x$ - and  $y$ -directions, respectively;  $k_w$  = permeability function (m/s);  $\rho_w$  = density of water ( $\text{Mg}/\text{m}^3$ );  $g$  = gravitational acceleration ( $\text{m}/\text{s}^2$ );  $m_w$  = coefficient of water volume change with respect to a change in matric suction ( $u_a - u_w$ );  $u_a$  = pore-air pressure (kPa), and  $t$  = time (second).

Equation 4 shows that the unbalanced flow of water through a soil element is equal to the change in water volume in the soil element. Unlike saturated soils, the permeability of an unsaturated soil is not constant (Fredlund and Rahardjo, 1993). The coefficient of permeability with respect to water for a soil is a non-linear function of the volumetric water content of the soil. When the soil approaches saturation, the permeability becomes constant and equal to the saturated coefficient of permeability with respect to water,  $k_s$ . In addition, the volumetric water content of the soil is dependent on the negative pore-water pressure in a non-linear fashion (soil-water characteristic curve or SWCC). In other words, the ability of the unsaturated soil to retain water varies with soil suction. SWCC follows different paths during drying and wetting (hysteresis) in nature where the soil on the drying path has a higher water content than the soil on the wetting path at a given matric suction.

## 2. METHODOLOGY

### 2.1 Field Instrumentation

The investigated slope in this study is located at the central part of Singapore within residual soil from Bukit Timah Granite. Figure 1 shows diagram of residual soil slope and the field instrumentation carried out in this study. The instrumentations can be divided into two parts; the first part was weather instrumentation for climatic data measurements while the second part was instrumentation for quantifying soil response to the flux boundary conditions. The monitoring period was one year (1<sup>st</sup> July 2016 to 30<sup>th</sup> June 2017).

The weather instrumentation includes tipping bucket rain gauge for rainfall, pyranometer for solar radiation, wind monitor for wind speed and direction, as well as temperature and relative humidity probes. The weather station for climatic data measurement was located near the toe. A 10 m high galvanized mast was erected on a concrete footing. The wind monitor, the solar panel, the lightning protection rod and the pyranometer were installed on top of the mast. The other instruments were installed at a height of 1 m from the ground surface together with the data logger. Soil temperature (ST) was measured at depths of 0.10m, 0.15m, 0.20m, and 0.25m.

The tensiometers (TM) and soil moisture sensors (SM) were installed within residual soil layer at depth of 2 m from crest and at distances 0.4 m; 2.4 m; 3.8 m and 4.6 m from slope face. The jet-fill tensiometers were calibrated properly prior to installation and then inserted into a tube to the specified depth. The reading from transducer was verified by a bourdon gauge attached to it. The

response of tensiometers to pore-water pressure change must be checked regularly to ensure the quality and physical performance of high air-entry ceramic tips. In this study, regular maintenance of the tensiometers was conducted twice a week by refilling the jet-fill reservoir with de-aired water and flushing the tensiometers to remove the accumulated or trapped air in the tubes caused by cavitation of water and air diffusion through the ceramic tip. Soil moisture sensor used in this study was of TDR type which was capable of measuring soil moisture up to saturation (0–100%) with accuracy of 1% and response time of 0.5 second. All soil moisture sensors were tested in water and air environment and their values corresponded to the values specified by manufacturer which was about 70 to 90% in pure water and zero in air.

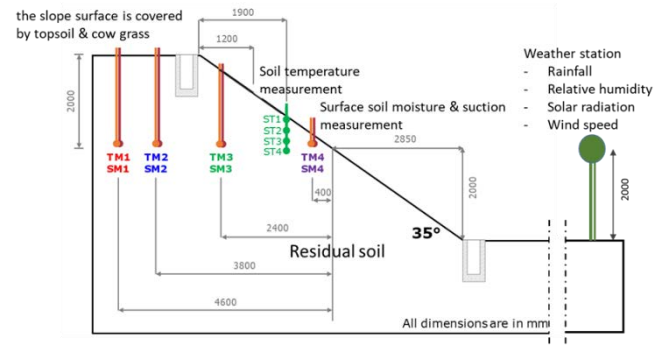


Figure 1 Plan view residual soil slopes with instrumentation locations

The readings of all measuring instruments were calibrated and checked before they were connected to a data acquisition system (DAS) to obtain instrumentation readings in real time. The data logger was powered by solar panel and battery. The cables were protected by corrugated tubing to prevent damages from rainfall and insects. The data logger recorded readings at a 10-minute interval regardless of rainfall events. The data logger sends all data through general packet radio service (GPRS) to a web page for remote monitoring. Figure 2 shows the weather station and data acquisition system used at the study site.



Figure 2 Data acquisition system used at the study site

### 2.2 Soil Properties

The slope was formed by residual soil with a thin layer of top soil as media for growing vegetative cover. The soil properties required for this study were investigated by performing laboratory tests on samples taken from the field. The grain size distribution shows that about 50% of the material is clay. The unified soil classification system USCS (ASTM D2487-00) categorized the soil to be highly plastic clay (CH). The bulk density of the residual soil was  $1.8 \text{ Mg}/\text{m}^3$ .

The saturated permeability of the soil was determined using the flexible-wall saturated permeability test (ASTM D5084-10). The saturated permeability of the soil is  $6 \times 10^{-7} \text{ m/s}$ . In order to perform analyses related to water flow in unsaturated soil, permeability functions of the soil need to be obtained. Permeability function can

be determined from the soil-water characteristic curve (SWCC) using a statistical method proposed by Childs and Collis-George (1950). The procedure for the prediction can be found in Fredlund and Rahardjo (1993). The SWCC of the soil in the site is obtained using Tempe cell and pressure plate according to ASTM D6838-02. The wetting and drying SWCCs of the residual soil are shown in Figure 3. The permeability functions obtained using the prediction method based on wetting and drying SWCCs are shown in Figure 4.

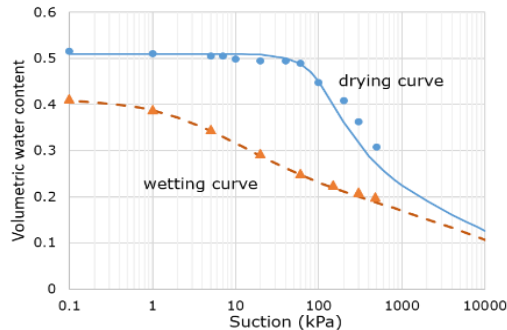


Figure 3 Drying and wetting SWCC of residual soil

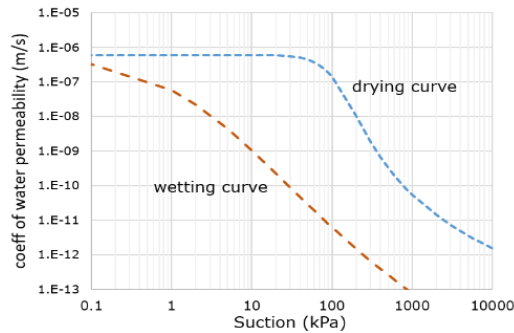


Figure 4 Drying and wetting permeability curve of residual soil

### 3. RESULTS AND DISCUSSION

#### 3.1 Rainfall

Figure 5 shows daily rainfall recorded from 1<sup>st</sup> July 2016 to 30<sup>th</sup> June 2017. The cumulative yearly rainfall was 2819 mm which is higher than the average annual rainfall in Singapore based on long term record from NEA Singapore (1981–2010) i.e. 2166 mm. The number of rainfall days during the monitoring period was 178 days, which was higher than the average annual number of rainfall days in Singapore (167 days). Rainfall monitoring at the study site indicates that the monthly rainfalls are quite different from the typical trend in Singapore as shown in Figure 6.

For example, the monthly rainfall in December 2016 (214.3 mm) was too low as compared to the mean monthly rainfall in Singapore for December 318 mm). On the other hand, the monthly rainfall in May 2017 (319 mm) was very high as compared to the average rainfall in Singapore for May (171 mm). The monthly rainfall in September, October and November 2016 were higher than the mean monthly rainfall for the months in Singapore. November 2016 was the wettest month during the monitoring period with 21 rainfall days accumulating to 311 mm rain and while August 2016 was the driest month with cumulative monthly rainfall of 98.6 mm. Figure 5 shows that the maximum daily rainfall occurred on 23<sup>rd</sup> January 2017 i.e. 103.8 mm. The month of January 2017 represented extreme condition because it started with a two-week dry period followed by very wet period towards the end of the month.

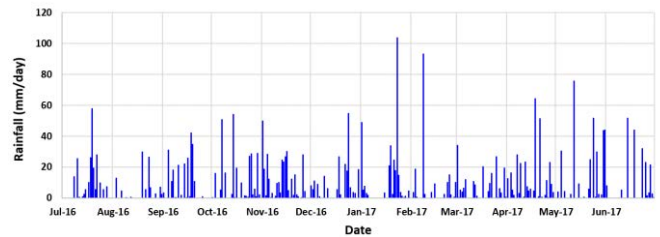


Figure 5 Daily rainfall from July 2016 to June 2017.

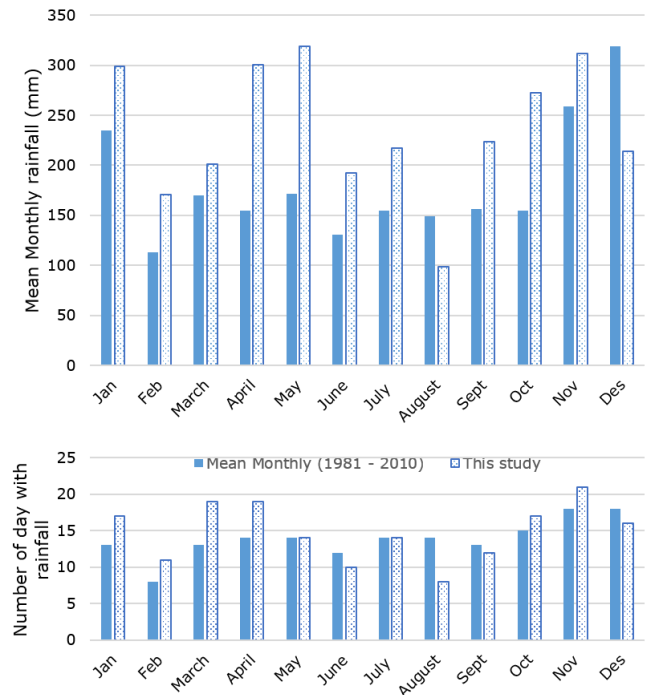


Figure 6 Mean monthly and number of rainfall days

#### 3.2 Climatic data

The climatic data observed from the weather station from July 2016 to June 2017 including air temperature ( $T_a$ ), relative humidity ( $RH$ ), solar radiation ( $SR$ ) as well as wind speed ( $W_s$ ) are shown in Figures 7. The climatic data obtained from the study site were also compared with the typical climatic data reported by NEA Singapore based on data from 1981 to 2010.

The minimum and maximum air temperature during the monitoring period was 22.9 and 36.9°C respectively. The range of air temperature was wider and higher than the mean range of air temperature in Singapore i.e. 23–33°C. As for the rainfall, the variation of air temperature during the monitoring period was different from the typical values recorded in Singapore. Both maximum and minimum temperature measured in this study occurred in January 2017. This is in accordance with the rainfall condition in which January 2017 represent an extreme condition. Past data indicated that the maximum temperature usually occur in March to May. In this study, the trend of higher temperature in March to May was overcome with heavy downpour (Figure 6).

Soil temperature was measured at depths of 0.10, 0.15, 0.20 and 0.25 m from ground surface. Field measurement performed in this study indicated that the soil temperature varies with depth and the time of the day. The least variation with the time of the day was obtained in the measurement of soil temperature at depth of 0.20 m from ground surface. Figure 7a shows the variation of soil temperature measured at depth 0.20 m as compared to maximum and minimum daily temperature. The soil temperature was lower in November, December and January, and higher in May, June and July.

Relative humidity plays an important role in the prediction of ET. The minimum and maximum relative humidity recorded in the study site were 67.4% to 99% with mean value of 80%. The recorded RH



was higher than the typical range recorded in Singapore i.e. 60 to 95%. Maximum relative humidity occurred in November due to high number of days with rainfall. The lowest relative humidity was recorded in August due to the least number of rainfall days. Figure 7b shows the maximum and minimum daily RH during the monitoring period.

The minimum and maximum solar radiation during the monitoring period was 1.12 and 14.76 MJ/m<sup>2</sup>/day respectively with mean value of 7.93 MJ/m<sup>2</sup>/day. These values are the typical of Singapore. The maximum solar radiation was recorded in the dry month of August 2016. The variation of solar radiation at the study site during the monitoring period is shown in Figure 7c.

The maximum wind speed (4.92 m/s) was recorded in February 2017. The recorded wind speed was lower than the range of wind speed in Singapore i.e. 0–13.375 m/s with mean value of 2.65 m/s. This may be because the location of the study site was surrounded by high rise buildings. The variation of wind speed throughout the year was also presented in Figure 7c.

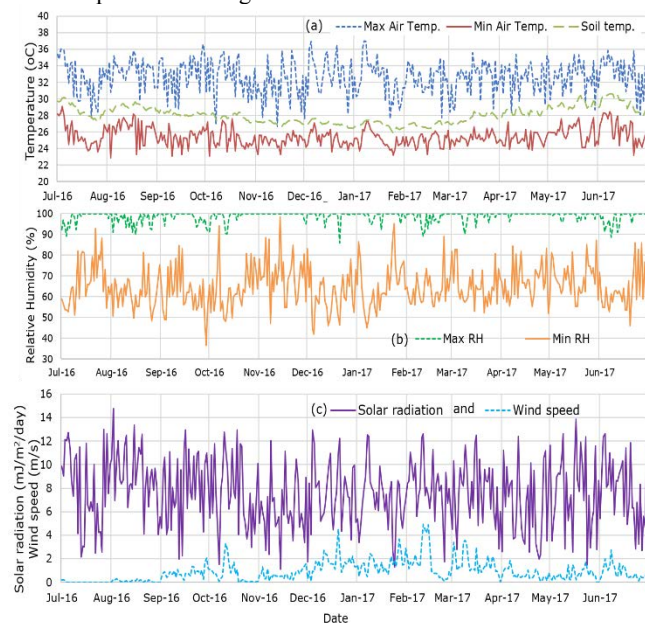


Figure 7 Variation of climate data from July 2016 to June 2017

### 3.2 Evapotranspiration

Figure 8 shows the  $ET_c$  calculated using FAO-Penman or FAO-56 Method for  $ET_o$  and coefficient of 1 for  $K_c$ , plotted together with rainfall data. The minimum, mean and maximum daily potential evaporation in the study area were 0.66, 1.92, and 3.26 mm respectively. These values are slightly less than reported by Rahardjo et al. (2017) based on their study in different part of Singapore. The minimum and maximum  $ET_c$  calculated in their study was 0.55 and 4.3 mm/day. The highest daily  $ET_c$  occurred in February and June 2017 while the lowest was in June. However, based on the monthly  $ET_c$ , the variation of  $ET_c$  follows weather variation on site. The highest monthly  $ET_c$  occurred in June (65.29mm) while the lowest was in November (47.77mm).

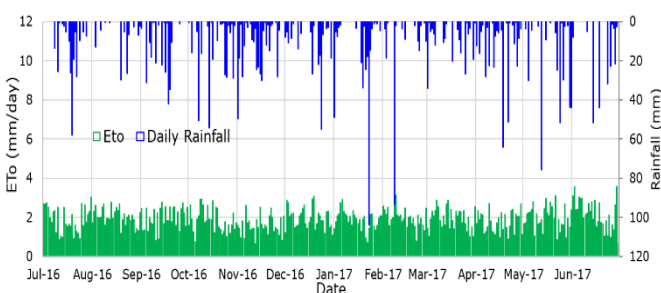
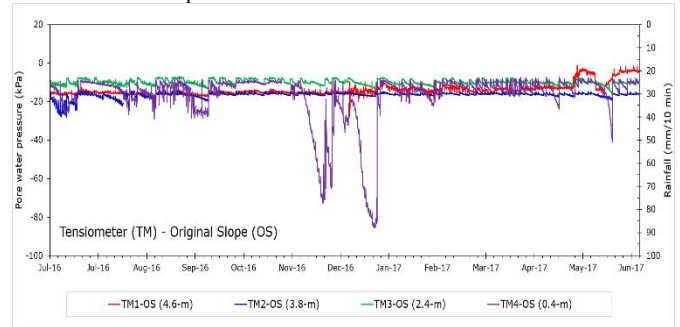


Figure 8 Evapotranspiration on slope surface at the study site from July 2016 to June 2017

### 3.3 Pore-water pressure measurements

The response of soil slope to rainfall and evapotranspiration from vegetated surface in terms of pore-water pressure is presented in Figure 9. The figure shows that the measurements at TM1 – TM3 were quite consistent, while measurements at TM4 varied significantly especially from November 2016 to January 2017. Based on the evaluation of rainfall and climatic data, this period represents extreme changes from dry to wet condition.

As shown in Figure 1, TM1 and TM2 have vertical distances of 2 m from crest while TM3 was 1.37 m below slope face. TM4 was very close to slope face i.e. 0.4 m horizontal distance or only 0.23 m vertical distance. Thus, TM4 is more affected by flux boundary conditions as compared to the other tensiometers.



\*Note: Refer to Figure 1 for instrumentation locations

Figure 9 Pore-water pressure recorded at the study site from July 2016 to June 2017

### 3.4 Soil's response to flux boundary conditions

Field data of pore-water pressure and volumetric water content throughout the monitoring period was plotted together with SWCC of residual soil in Figure 10. It can be seen that measurements by TM1-SM1, TM2-SM2 and TM3-SM3 were plotted well within the hysteretic of the SWCC. The range of suction was quite narrow i.e. 4 – 27 kPa. The volumetric water content ranged from 27% to the saturated volumetric water content of the soil (51%). This shows that the measurements at TM1 to TM3 are representative of the residual soil forming the slope. On the other hand, the measurement by TM4 below the SWCC wetting curve of the residual soil. It was deduced that the soil response at TM4-SM4 is more representative of top soil instead of the residual soil.

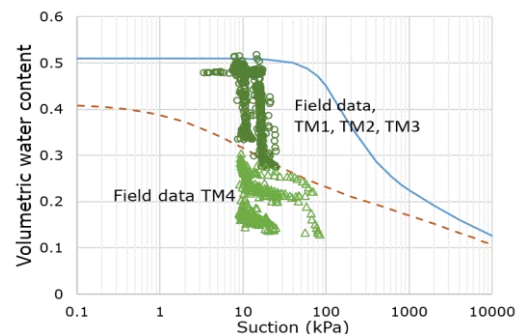


Figure 10 Plot of pore-water pressure and volumetric water content measured at the study site from July 2016 to June 2017 in SWCC of residual soil.

Soil samples were collected from the slope surface to a depth of 20 cm. SWCC and saturated permeability tests were carried out on the samples using the same procedure as for the residual soil. It was found that the saturated volumetric water content of the top soil was lower than that of the residual soil. The top soil has lower density as compared to the residual soil, thus the higher void ratio shifted the SWCC to the left, resulting in a lower air-entry value. The saturated

coefficient of permeability of the top soil was  $1 \times 10^{-5}$  m/s which is higher than that of the residual soil ( $6 \times 10^{-7}$  m/s).

The field data from TM4-SM4 were plotted on the SWCC curves of the top soil as shown in Figure 11. The figure shows that the field data could be plotted well inside the hysteresis of the SWCC of the top soil. The range of suction was i.e. 8 – 90 kPa, while the range of volumetric water content was from 13 to 30%. The maximum volumetric water content was less than the saturated volumetric water content of the surface soil. It may be attributed to some water intercepted by vegetation (grass) at the surface. The same reason that the evapotranspiration (*ET*) is less than the actual evaporation (*AE*) from base soil surface.

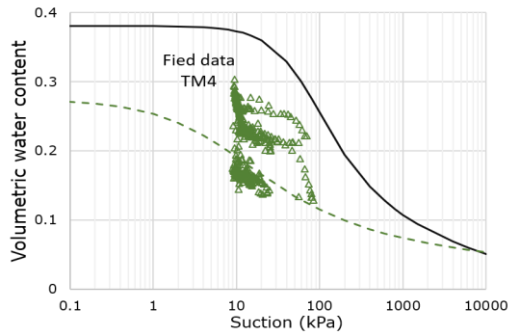


Figure 11 Plot of pore-water pressure and volumetric water content measured by TM4 from July 2016 to June 2017 in SWCC of top soil.

#### 4. CONCLUSIONS

Field measurements of flux boundary conditions and soil response were carried out in a residual soil slope at the central part of Singapore. The measurements presented in Figures 5 and 7 specified that the seasonal variation of rainfall was quite different from the typical trend in Singapore (Figure 6). The dissimilar trend also observed for the other flux boundary conditions such as air temperature and relative humidity. Highly variable conditions occurred during the months of December 2016 and January 2017. This could be identified by unusually high air temperature and long period of dry condition which are different from the normal conditions in Singapore. The long dry period allowed high pore-water pressure to be recorded by TM4 which is located closest to the ground surface (Figure 9).

Readings of pore-water pressure and soil water content recorded by TM1-SM1, TM2-SM2, TM3-SM3 are representative of the SWCC of the residual soil. Thus, the readings are representative of the soil where the instrumentations were installed. However, the plot for TM4-SM4 located at vertical distance of 23 cm from ground surface was more representative of top soil which has lower density and higher coefficient of permeability. This showed that the readings of instrumentation closer to the ground surface was affected by the flux boundary conditions and the consistency of surface soil as well as vegetative cover.

#### 4. REFERENCES

ASTM D5084-10 Standard Test Method for Measurement of Hydraulic Conductivity of Saturated Porous Material using a Flexible Wall Permeameter, ASTM International, West Conshohocken. PA.

ASTM D6838-02 Standard Test Method for Determination of SWCC for Desorption using Hanging Column, Pressure Extractor, Chilled Mirror Hygrometer or Centrifuge, ASTM International, West Conshohocken. PA.

ASTM D 2487-00 Standard Practice for Classification of Soils for Engineering Purposes (Unified Soil Classification System) , ASTM International, West Conshohocken. PA.

Allen R.G., Pereira L.S., Raes D., Smith M. (1998) Crop evapotranspiration: guidelines for computing crop water requirements Food and Agriculture Organization of the United Nation, Rome.

Blight G.E. (1997) The “Active” Zone in Unsaturated Soil Mechanics. 1st GRC Lecture, Nanyang Technological University, Singapore.

Childs E.C., Collis-George G.N. (1950) “The permeability of porous materials”. Proc. Royal Society of London 210A. pp. 392-405.

Chipp, P.N., Henkel, D.J., Clare, D.G. & Pope, R.G. (1982) Field Measurement of Suction in Colluvium Covered Slopes in Hong Kong. Proc. 7<sup>th</sup> Southeast Asian Geotechnical Conf., Hong Kong, pp.49-62.

Fredlund D.G., & Xing A. (1994) “Equations for the Soil-Water Characteristic Curve”. Canadian Geotech. Journal 31 pp. 521-532.

Fredlund, D. G. & Rahardjo, H. (1993). Soil Mechanics for Unsaturated Soils. New York: John Wiley & Sons, Inc.

Joel, A., Messing, I., Seguel, O., & Casanova, M. (2002) “Measurement of surface water runoff from plots of two different sizes”. Hydrological Processes. 16(7) pp. 1467-1478.

Lazzara P. & Rana G. (2010) “The use of crop coefficient approach to estimate actual evapotranspiration: a critical review for major crops under Mediterranean climate”. Italian Journal of Agrometeorology 2 pp. 25-39.

Lee, M.L. Gofar N. & Rahardjo H. (2009) “A Simple Model for Preliminary Evaluation of Rainfall-Induced Slope Instability. Engineering Geology”. 108(3-4) pp. 272-282.

Li, A.G., Yue, Tham, L.G. and Lee C.F., (2005) “Field-monitored variations of soil moisture and matric suction in a saprolite slope”. Canadian Geotechnical Journal. 42, pp. 13-26.

Gasmo, J.M., Rahardjo, H. and Leong, E.C. (2000) “Infiltration Effects on Stability of a Residual Soil Slope”. Computer and Geotechnics, 26, April, pp.145-165.

Gitirana Jr., G., Fredlund, D.G., Fredlund, M. (2006) “Numerical modeling of soil-atmosphere interaction for unsaturated surfaces”. Proc. 4<sup>th</sup> Intl. Conf. Unsaturated soils, US., pp.658-669.

Gitirana Jr., G., Fredlund, D.G., Fredlund, M. (2005) “Infiltration-runoff boundary conditions in seepage analysis”. Proc. 58<sup>th</sup> Canadian Geotech. Conf. Canada, pp.516-523.

Gofar N. Lee, M.L. & Kassim, A. (2008) “Response of Suction Distribution to Rainfall Infiltration in Soil Slope”. Electronic J. of Geotechnical Engineering. 13 (E), pp.1-13

Ng, C.W.W., Springman, S.M. and Alonso E.E. (2008). “Monitoring the Performance of Unsaturated Soil Slopes”. Geotechnical and Geological Engineering. 26(6), pp.799-816.

Ng, C.W.W., Zhan, L.T., Bao, C.G., Fredlund, D.G. and Gong, B.W., (2003) “Performance of an Unsaturated Expansive Soil Slope Subjected to Artificial Rainfall Infiltration”. Géotechnique. 53(2), pp. 143-157.

Penman, H.L (1948) “Natural evapotranspiration from open water, bare soil and grass”. Proc. Royal Society London Ser. A.193, pp.120-145.

Rahardjo, H., Amalia, N., Leong, E.C. Harnas, F.R. Lee, T.T. and Fong, Y.K. (2017) “Flux Boundary Measurements for the study of Tree Stability”. Landscape Ecol Eng. 13:81-92

Rahardjo, H., Satyanaga, A. Harnas, F.R. and Leong, E.C. (2014) “Comprehensive Instrumentation for Real Time Monitoring of Flux Boundary Conditions in Slope” Proc. 3<sup>rd</sup> Italian Workshop on Landslides, Italy.

Rahardjo, H., Satyanaga, A. and Leong, E.C. (2013). “Effects of Flux Boundary Conditions on Pore-water Pressure Distribution in Slope”. Engineering Geology, 165, October, pp. 133-142.

Rahardjo, H., Lee, T.T. Leong, E.C. and Rezaur, R.B. (2005). “Response of a Residual Soil Slope to Rainfall”. Canadian Geotechnical Journal, 42(2), pp. 340-351.

Rahardjo, H., Leong, E.C., Gasmo, J.M. and Tang, S.K. (1998) “Assessment of rainfall effects on stability of residual soil

- slopes". Proc. 2<sup>nd</sup> Intl. Conf. Unsaturated Soils, China, pp. 280-285.
- Sattler, P.J. & Fredlund, D.G. (1991). "Modelling vertical ground movements using surface climatic flux". Proc. Geotechnical Engineering Congress, US., pp. 1292-1306.
- Yunusa, G.H. Kassim, A. & Gofar, N. (2014) "Effect of Surface Flux Boundary Conditions on Transient Suction Distribution in Homogeneous Slope". Indian J. Science & Technology, 7(12), 2064–2075
- Zotarelli L, Dukes MD, Romero CC, Migliaccio KW, Morgan KT (2009) Step by step calculation of Penman-Monteith evapotranspiration (FAO-56 Method), University of Florida.